

This is the accepted manuscript made available via CHORUS. The article has been published as:

## Material- and geometry-independent multishell cloaking device

Pattabhiraju C. Mundru, Venkatesh Pappakrishnan, and Dentcho A. Genov

Phys. Rev. B **85**, 045402 — Published 3 January 2012

DOI: [10.1103/PhysRevB.85.045402](https://doi.org/10.1103/PhysRevB.85.045402)

# Generic Cloaking Device

Pattabhiraju C. Mundru, Venkatesh Pappakrishnan and Dentcho A. Genov\*  
College of Engineering and Science, Louisiana Tech University, Ruston, LA 71270, USA

In this paper we proposed a multi-shell generic cloaking system. A transparency condition independent of the object's optical and geometrical properties is proposed in the quasi-static regime of operation. The suppression of dipolar scattering is demonstrated in both cylindrically and spherically symmetric systems. A realistic tunable-low loss shell design is proposed based on composite metal-dielectric shell. The effects due to dissipation and dispersion on the overall scattering cross-section are thoroughly evaluated. It is shown that a strong reduction of scattering by a factor of up to  $10^3$  can be achieved across the entire optical spectrum. Full wave numerical simulations for complex shape particle are performed validating the analytical theory. The proposed design does not require optical magnetism and is generic in the sense that it is independent of the object's material and geometrical properties.

\*Author to whom correspondence should be addressed. Email address: dgenov@latech.edu

## I. INTRODUCTION

Recently, *cloaking or invisibility* has received significant attention from the scientific community. Several methods have been proposed to cloak macroscopic and microscopic objects: transformation optics (TO)<sup>1-12</sup> and elimination of dipolar scattering<sup>17-19</sup> are widely used. Both of these approaches are based on engineering a specific material shell(s) around an object to render it invisible for external observers.

In 2006, Leonhardt<sup>3</sup> used optical conformal mapping to design an isotropic cloaking design with spatially dependent refractive index around an object, achieving invisibility in the ray approximation. Pendry *et al.*<sup>4</sup> proposed the TO approach in order to design an electromagnetic metamaterial (EMM) shell that bends light rays and conformably transfers the wave fronts around an object. Using TO, Lai *et al.*<sup>7</sup> designed a complementary media<sup>8</sup> that can conceal objects placed at distance outside the cloaking system from electromagnetic radiation. McCall *et al.*<sup>10</sup>, by transforming both space and time reported a spacetime cloak (STC) design that can hide events rather than objects. In contrast to spatial transformation cloaks which bend light around a finite region of space, STC works on the variation of the velocity of light before and after the occurrence of the event to be cloaked and its realization demands sophisticated temporal EMM designs. The EMMs are artificial materials engineered with desired electromagnetic properties that are difficult or impossible to find in nature. The remarkable properties of these materials are responsible for developing novel optical systems with negative refractive index media<sup>13</sup>, lensing with super resolution<sup>14</sup>, cloaking devices<sup>11</sup>, systems that creates an optical illusion such that an object can appear to external observe with entirely different characteristics<sup>15</sup>. Furthermore, EMMs have been used to mold the flow of light at will<sup>16</sup>, functionalities that are virtually impossible to achieve with naturally available materials.

Electromagnetic invisibility through elimination of dipolar scattering was studied decades ago by Kerker *et al.*<sup>18</sup> in the case of a sub-wavelength ellipsoidal objects. More recently, a similar study in the case of spherical and cylindrical geometries was presented by Alù *et al.*<sup>17</sup>. In these studies a reduction in the total scattering cross-section was demonstrated by using dielectric shells with appropriately configured geometrical and optical properties. Zhou *et al.*<sup>19</sup> furthered this concept by using the idea of *neutral inclusion* to derive the generalized transparency condition in quasi-static limit. However, all these studies place explicit geometrical and material constraints upon the shells of the cloaking system as well as the object. These constraints make the cloak crucially dependent on the optical and geometrical properties of the object and arguably limit its applicability.

In this paper, we propose a multi-shell design that can cloak an object regardless of its shape and material (optical) properties in the quasi-static regime. A set of transparency conditions independent of the object are derived for both cylindrically and spherically symmetric systems. Most importantly, as a material realization of our system, we propose a *zero index-lowloss-tunable* shell design based on metal-dielectric composite materials. Our results show that the proposed design can achieve cloaking across the entire optical spectral range and can decrease the scattering-cross section by a factor up to  $10^3$ . In addition, full wave analysis performed for a two dimensional or cylindrically symmetric system shows the object independence of the design in good agreement with the developed analytical theory.

The rest of the paper is organized as follows. Section II outlines the transparency conditions for a multi-shell cloaking system independent of the object optical and geometrical properties. Section III analyses the behavior of the cloak based on realistic shells *i.e.*, shells made of dispersive materials (bulk metal and metal-dielectric composites), and compares the results to

the ideal lossless case. Section IV provides a time varying and finite element frequency domain (FDFD) analysis of our cloaking system, respectively.

## II. THEORETICAL ANALYSIS

The geometry of the problem is depicted in Fig. 1. An object of arbitrary shape and permittivity  $\varepsilon_0$  is placed inside a cylindrical or spherical domain of radius  $r_0$  (core) surrounded by a system of  $l$  shells of radii  $r_1, r_2, \dots, r_l$  ( $r_0 < r_1 < r_2 \dots r_l$ ) and permittivities  $\varepsilon_1, \varepsilon_2, \dots, \varepsilon_l$ , respectively. The cloak is embedded in a medium with permittivity  $\varepsilon_e$  and illuminated by a uniform electric field  $E_0$  polarized along  $+x$  axis (or transfer magnetic (TM) wave). In the quasi-static limit, the electric potential inside and outside the cloak can be written as:

$$\varphi_{2D} = E_0 \sum_{n=1}^{\infty} (A_n^{2D} r^n + S_n^{2D} r^{-n}) \cos(n\phi), \quad (1)$$

$$\varphi_{3D} = E_0 \sum_{n=1}^{\infty} (A_n^{3D} r^n + S_n^{3D} r^{-(n+1)}) P_n(\cos(n\phi)), \quad (2)$$

where  $A_n^d, S_n^d$  are amplitude coefficients,  $P_n$  are the associated Legendre polynomials and  $d$  is the dimensionality. On applying tangential and normal boundary conditions at  $r_0, r_1, r_2, \dots, r_l$ , the dipolar terms ( $n = 1$ ) responsible for the far field scattering in the embedding media can be written as

$$S_1^d = r_l^d \frac{\varepsilon_{eff}^l - \varepsilon_e}{\varepsilon_{eff}^l + (d-1)\varepsilon_e}, \quad (3)$$

where

$$\varepsilon_{eff}^l = \varepsilon_l + \frac{d\varepsilon_l p_l (\varepsilon_{eff}^{l-1} - \varepsilon_l)}{d\varepsilon_l + (1-p_l)(\varepsilon_{eff}^{l-1} - \varepsilon_l)}, \quad (4)$$

is effective permittivity of the  $l$ -shell system, and  $p_l = (r_{l-1}/r_l)^d$  are the shells surface/volume ratios. We must note that using the natural condition  $\varepsilon_{eff}^0 = \varepsilon_0$ , Eqs. (3) and (4) provide a

straightforward recurrence formula for estimating the scattering coefficient of multilayered dielectric particles in the quasi-static approximation without explicitly solving the boundary value problem (see Appendix for more details). This rendering of the problem also gives an intuitive understanding of the scattering process as that of an equivalent spherical/cylindrical particle with effective permittivity  $\varepsilon_{eff}^l$  immersed in a host environment with permittivity  $\varepsilon_e$ .

Alù *et al.* and Zhou *et al.*<sup>17, 19</sup> have shown that, in the quasi-static limit, complete elimination of dipolar scattering can be achieved by a proper choice of the shell(s) radii. Following their hypothesis, in the limit  $S_1^d \rightarrow 0$  ( $\varepsilon_{eff}^l = \varepsilon_e$ ) we obtain a general transparency condition for  $l$  –shell cloaking system which depends on the object permittivity and size:

$$p_l = \left( \frac{\varepsilon_l - \varepsilon_e}{\varepsilon_l - \varepsilon_{eff}^{l-1}} \right) \left( \frac{\varepsilon_{eff}^{l-1} + (d-1)\varepsilon_l}{\varepsilon_e + (d-1)\varepsilon_l} \right), \quad (l \geq 1), \quad (5)$$

The condition in Eq. (5) is consistent with the transparency conditions reported in<sup>17, 19</sup> for single-shell and two-shell geometries. Specifically, for  $l = 1$  and  $d = 3$  *i.e.*, a single shell spherically symmetric cloak, Eq. (5) reduces to the condition reported by Alù *et al.* [7]

$$p_1 = \left( \frac{r_0}{r_1} \right)^3 = \frac{(\varepsilon_1 - \varepsilon_e)(2\varepsilon_1 + \varepsilon_0)}{(\varepsilon_1 - \varepsilon_0)(2\varepsilon_1 + \varepsilon_e)}, \quad (6)$$

where  $\varepsilon_1$  is the shell permittivity. As evident from Eq. (6) this design does not require high refractive indices or optical magnetism as in the case of transformational optics (TO)<sup>12</sup>. However, realizations of such cloaking systems present a serious disadvantage; redesign of the entire cloak is necessitated for any change in the object's properties ( $\varepsilon_0$  and  $r_0$  are the permittivity and radius of the object), and it is applicable only for spherically/cylindrically symmetric objects.

Alternatively, here we propose a different condition to achieve complete elimination of dipolar scattering for a cloak with  $l \geq 2$  shells. By inspection (see Eqs. (3) and (4)) this is

107 achieved ( $\varepsilon_{eff}^l = \varepsilon_e$ ), if the two outermost cloaking shells have permittivities that satisfy the  
 108 following conditions

$$\varepsilon_{l-1} = 0, \quad \varepsilon_l = \varepsilon_e \frac{1 + p_l/(d-1)}{1 - p_l}. \quad (7)$$

109 Provided a zero index material can be designed the permittivity of the outermost shell is  
 110 dependent only on the radii of the  $l^{th}$ , and  $(l-1)^{th}$  shells which is in sharp contrast with the  
 111 transparency condition given by Eqs. (5), and (6). Thus, in the quasi-static limit, a cloaking  
 112 system parameterized by the transparency condition Eq. (7) has the potential to cloak objects  
 113 with arbitrary optical properties. Furthermore, as will be demonstrated in Section IV, the  
 114 conditions  $\varepsilon_{l-1} \rightarrow 0$ , allows cloaking of objects with arbitrary shapes provided it is immersed  
 115 within shells of order lower than  $l-1$ . Interestingly, a striking similarity exists between the  
 116 cloak designs based on our approach and those on conventional transformation optics. In the case  
 117 of transformation optics, perfect cloaking can be achieved provided the permittivity or/and  
 118 permeability of the anisotropic shell is zero at the boundary between the shell and the object<sup>6</sup>.  
 119 Zero index materials correspond to a situation where the local electromagnetic field do not  
 120 experience phase shift as it travels through the material. In the case of cloaking this also implies  
 121 a singular value of the local wavelength ( $\lambda \rightarrow \infty$ ) or an effective size of the object equal to zero.  
 122 This explain why in the case of transformation optics and under the here proposed transparency  
 123 condition Eq. 7, the invisibility devices operate independent of the object geometrical or/and  
 124 material properties. An object with effective size equal to zero does not interact with the  
 125 impinging light. For the here proposed cloak, the simplest realization is the two-shell design.

### III. CLOAK DESIGN AND TUNABILITY

#### A. Metallic shell design

We consider a two shell cylindrical and spherical cloaking systems (see Fig. 1(b) and 1(c)) with air ( $\varepsilon_e = 1$ ) as environment. To satisfy the transparency condition Eq. (7) we utilize a metallic inner shell. The metal permittivity is described by the Drude model,  $\varepsilon_m(\omega) = \varepsilon'_m(\omega) + i\varepsilon''_m(\omega) = \varepsilon_b - \omega_p^2/\omega(\omega + i\omega_\tau)$ , where  $\omega_p$  is plasma frequency,  $\omega_\tau$  is relaxation rate and  $\varepsilon_b$  is contribution due to interband transitions. Clearly, at the modified plasma frequency  $\tilde{\omega}_p = \omega_p/\sqrt{\varepsilon_b}$ , the metal permittivity  $\varepsilon'_m(\tilde{\omega}_p) = 0$  (for  $\omega_\tau/\tilde{\omega}_p \ll 1$ ) and a metal shell can be used to implement the clock. To characterize the clock performance we define the relative scattering length (RSL), for the cylindrical case  $d = 2$ , and relative scattering cross-section (RSCS) for spherically symmetric case  $d = 3$  as

$$\sigma_R^d = \frac{\sigma_{cloak}^d}{\sigma_{object}^d} = \frac{|S_{1,cloak}^d|^2}{|S_{1,object}^d|^2}, \quad (8)$$

where  $\sigma_{cloak}^d$  and  $\sigma_{object}^d$  are the scattering length (scattering-cross section) of the cloak and object, respectively. Substituting the transparency condition Eq. (7) in Eq. (3) and using  $\varepsilon_2 = \varepsilon_m(\tilde{\omega}_p) = i\varepsilon''_m(\tilde{\omega}_p)$  (here  $\varepsilon''_m$  is the imaginary part of the metal permittivity), in the second order of the small parameter  $\varepsilon''_m \approx \varepsilon_b \omega_\tau/\tilde{\omega}_p \ll 1$  we obtain

$$\sigma_R^d(\tilde{\omega}_p) \approx \left( \frac{d\varepsilon''_m(\tilde{\omega}_p)}{p_1} \right)^2 \left( \frac{(\varepsilon_0 + d - 1)(1 + (d - 1)p_1)}{(\varepsilon_0 - 1)(1 - p_1)(p_2 + d - 1)^2} \right)^2. \quad (9)$$

The existence of material dissipation clearly affects the cloak performance with  $\sigma_R^d \approx (\omega_\tau/\omega_p)^2$  increasing quadratically with the relaxation rate  $\omega_\tau$ . Furthermore inspection of Eq. (9) shows that a geometrical optimization could be archived with the scattering having a minimum for  $p_1 =$



144  $1/(1 + \sqrt{d})$ . Finally, using Eq. (7) the optimal RSL/RSCS can be written as function of the outer  
 145 shell permittivity

$$\sigma_{R,min}^d(\tilde{\omega}_p) \approx \varepsilon_b^3 \left( \frac{\omega_\tau}{\omega_p} \right)^2 \left( \frac{(\varepsilon_0 + d - 1)(d - 1 + 1/\varepsilon_2)^2}{d(\varepsilon_0 - 1)(1 - \sqrt{d})^2} \right)^2. \quad (10)$$

146 To demonstrate the cloak performance we consider two separate designs for the  
 147 cylindrical and spherical geometries. Due to lower dissipative losses, we chose silver with  
 148  $\hbar\omega_p = 9.1\text{eV}$ ,  $\hbar\omega_\tau = 0.02\text{eV}$  and  $\varepsilon_b = 5$ .<sup>22</sup> The cloak's performances calculated as a function  
 149 of the outer shell permittivity  $\varepsilon_2$  are shown in Fig. 2. For comparison, we include the RSL/RSCS  
 150 of the ideal systems (without dissipative losses) and with a silver inner shell. The RSL/RSCS of  
 151 the ideal systems approaches zero, implying *perfect invisibility* at the outer shell permittivity  
 152 values  $\varepsilon_2 = 5$  and  $\varepsilon_2 = 10$  in cases I and II (see Fig. 2), for cylindrical and spherical geometries.  
 153 These results are in excellent agreement with the values predicted by the transparency condition  
 154 Eq. (7). A significant reduction in scattering for the metal shell systems are also observed at the  
 155 predicted outer shell dielectric permittivities  $\varepsilon_2$  (see Fig. 2, dashed lines). In the figures we have  
 156 also included the minimal RSL and RSCS as given by Eq. (10), providing a guideline of the  
 157 maximal affects that can be achieved with proposed design. At the optimal outer shell  
 158 permittivity the exact result correlates well with the predicted values, and for strongly scattering  
 159 objects ( $\varepsilon_0 \rightarrow \infty$ ) asymptotically approaches the limit  $\sigma_{RSCS}^{min} \rightarrow \varepsilon_b^3 (\omega_\tau/\omega_p)^2 (1 + 1/\sqrt{d})^4 \ll 1$ .  
 160 Finally, we must note that the cloak based on the metal shell design has inherently a rather  
 161 narrow frequency range of operation. The operation range  $\omega \in (\tilde{\omega}_p - \Delta\omega, \tilde{\omega}_p + \Delta\omega)$  is roughly  
 162 set by the condition  $|\varepsilon'_m(\tilde{\omega}_p \pm \Delta\omega)| = \varepsilon''_m(\tilde{\omega}_p \pm \Delta\omega)$ , which gives  $\Delta\omega = \omega_\tau/2$ .

## B. Composite media: optical tunability

From the discussions in the previous subsection it is clear that while metal shells can be used to provide substantial reduction in scattering at the respective modified plasma frequencies their response cannot be tuned to operate across a broader spectral range. However such tunability can be achieved using nano-composite materials realized by embedding metal inclusions of permittivity  $\epsilon_m$  in a dielectric host with permittivity  $\epsilon_h$ .<sup>1, 12, 23</sup> If the inclusions are randomly oriented ellipsoids with small volume fraction  $f$ , the effective permittivity of the composite is given by the Maxwell-Garnett formula<sup>24-27</sup>

$$\epsilon_{eff} = \epsilon_h + \frac{f}{3} \sum_{j=x,y,z} \frac{\epsilon_h(\epsilon_m - \epsilon_h)}{\epsilon_h + \eta_j(\epsilon_m - \epsilon_h)} \quad (11)$$

where  $\eta_j$  are the depolarization factors of the ellipsoids satisfying the condition  $\sum_{j=x,y,z} \eta_j = 1$ . For prolate spheroids (needle shaped) *i.e.* ellipsoids with semi-axes  $a > b = c$ , the depolarization factor is given as

$$\eta_x = \eta = \frac{1 - e^2}{e^2} \left( \frac{1}{2e} \ln \left( \frac{1 + e}{1 - e} \right) - 1 \right), \quad (12)$$

where  $e^2 = 1 - (b/a)^2$  is the eccentricity.<sup>25</sup> The other two depolarization factors are equal and given by  $\eta_y = \eta_z = (1 - \eta)/2$ .

To operate at reduced losses and simplify the design we consider only the ellipsoid's low frequency resonance set by the condition  $\epsilon'_m(\omega) = -\epsilon_h(1 - \eta)/\eta$ . The effective permittivity of the composite depends on the physical and geometrical properties of the spheroids, which allows for substantial flexibility in satisfying the transparency condition in Eq. (7). Since Eq. (11) is valid for small volume fractions, usually less than 5%, we study the effects due to change in the depolarization factor, *i.e.* the shape of the inclusions or the host material of the composite, or

both. For small metal losses ( $\varepsilon''_m/\varepsilon'_m \ll 1$ ), the depolarization factor that satisfies the transparency condition  $\varepsilon'_{eff}(\omega_{op}) = 0$  can be written as

$$\eta = \frac{1}{1 - \varepsilon'_m(\omega_{op})/\varepsilon_h} - \frac{f}{3}, \quad (13)$$

where  $\omega_{op}$  is the operation frequency, and the depolarization factor must vary from  $\eta = 0$  (needles) to  $1/3$  (spheres). Concurrently, the operation frequency for a given depolarization factor is obtained as  $\omega_{op} = \omega_p / \sqrt{\varepsilon_b - \varepsilon_h + 3\varepsilon_h/(3\eta + f)}$ . We must note that Eq. (13) is only valid for  $f > 6\varepsilon_h\varepsilon''_m/[(\varepsilon''_m)^2 + (\varepsilon_h - \varepsilon'_m)^2]$ , and for lower concentrations the transparency condition cannot be satisfied ( $\varepsilon'_{eff} > 0$ ).

The operation frequency range of the composite cloak is depicted in Fig. 3(a). For air as a host medium and tuning the depolarization factor of the ellipsoids the frequency range of operation is  $\hbar\omega_{op} \in (1.14 - 3.89)$  eV. For the same ellipsoid volume fraction and glass as a host medium the operational frequency exhibits a red shift and is within the range  $\hbar\omega_{op} \in (0.83 - 3.74)$  eV. Clearly, by varying the composite host material and ellipsoidal aspect ratio (depolarization factor), one can tune the operation frequency over large sections of the visible and near-infrared spectra. However, for low depolarization factors the spheroid aspect ratios become prohibitive pertaining to the design of the cloak (the physical size of the system should be smaller than the incident wavelength) and one should impose the restriction  $1/3 \geq \eta > 1/10$ , which corresponds to ellipsoid aspect ratios within the range  $1 \leq a/b < 3$ . This restriction is sufficiently weak enough to allow effective cloaking throughout the entire optical spectral range.

To estimate the RSL /RSCS of the composite cloak we rely on Eq. (9) with the substitution  $\varepsilon'_m \rightarrow \varepsilon''_{eff}(\omega_{op})$ , where the composite effective permittivity is obtained from Eq. (11) and (13) and is given as

$$\varepsilon_1 = i\varepsilon''_{eff}(\omega_{op}) = \frac{3\varepsilon_h^2}{f} \frac{i\varepsilon''_m}{(\varepsilon_h - \varepsilon'_m)^2} \quad (14)$$

For the geometrically optimized design (with  $p_1 = 1/(1 + \sqrt{d})$ ), low frequency of operation and strongly scattering objects ( $\varepsilon_0 \rightarrow \infty$ ) the RSCS/RSL asymptotically approaches the limit

$$\sigma_{R,min}^d(\omega_{op}) = \left( \frac{3\omega_\tau \omega_{op} \varepsilon_h^2}{f \omega_p^2} \right)^2 \left( \frac{1 + \sqrt{d}}{\sqrt{d}} \right)^4 \quad (15)$$

Figures 3(b) and 3(c) depict the RSCS/RSL vs. the outer-shell permittivity ( $\varepsilon_2$ ) for two-shell cylindrical and spherical cloaking systems with inner-shells made of different metal dielectric composites. We also compare with the ideal case (non-dispersive media) and include air (dotted line) and glass (dashed line) as the composite host materials. The operation frequency for all cases is set at  $\hbar\omega = 1.14$  eV. A strong reduction in the scattering/extinction is observed, with the composite design based on air as a host media showing better performance (as expected by Eq. (15)). Furthermore, a reduction of about 40% is observed as compared to the cloak designs based on bulk metal inner shells (see Fig. 2). Again the minimal RSCS and RSL are obtained at outer-shell permittivity ( $\varepsilon_2$ ) corresponding to the transparency condition Eq. (7). In the figures we also include the predicted geometrically optimized results as per Eqs. (9) and (14), which closely match the minimal values due to the exact calculations.

Finally, to provide a complete picture of the cloaks performance, in Figs. 4(a) and 4(b) we vary the outer shell permittivity ( $\varepsilon_2$ ) and operational frequency ( $\omega_{op}$ ), respectively. A substantial decrease in the RSL and RSCS are observed across the entire optical and near infrared spectral range. As predicted by Eq. (15), the scattering increases with increasing frequency to the point where the effect of the shell on the scattering cross-section is no longer beneficial (for  $\sigma_{R,min}^d > 1$  and  $\hbar\omega_{op} > 3.2$  eV). We should note that further decrease in

scattering may be achieved by increasing the volume fraction of the spheroids provided the applicability of Eq. (11) is not violated.

#### IV. FULL WAVE ANALYSIS OF A GENERIC CYLINDRICAL CLOAK

The transparency condition Eq. (7) proposed in this work is valid for small objects, i.e. those whose physical size is much smaller than the wavelength of the impinging light. If the object size is comparable to the incident wavelength, the quasi-static analysis is no longer valid and the transparency condition is expected to fail. To study this transition and better understand the limiting system sizes of the design we perform a full wave analyzes of a cylindrical two shell cloak at optical and near infrared frequencies.

We consider scattering of a plane transfer magnetic (TM) wave by an infinite two shell cylindrical cloak as depicted in Fig. 1(b). The components of the incident  $H_z^i$  and scattered  $H_z^s$  magnetic fields outside the cloak assume the following well known general form

$$H_z = H_z^i + H_z^s = H_0 \sum_{n=-\infty}^{\infty} i^n [J_n(k_e r) + S_n H_n^1(k_e r)] e^{in\phi}, \quad (16)$$

where  $J_n$ ,  $H_n^1$  are the Bessel and Henkel functions of the first kind, respectively,  $k_e = (\omega/c)\sqrt{\epsilon_e}$  is the wave vector in the host medium, and  $S_n$  are the scattering coefficients determined by applying the respective boundary conditions (see Appendix). The scattering cross-length is then given as a sum over all multipoles<sup>28-30</sup>

$$\sigma = \frac{4}{k_e} \sum_{n=-\infty}^{\infty} |S_n|^2. \quad (17)$$

In the calculations, the geometrical parameters of the cloak are set at the optimal value  $p_1 = 1/(1 + \sqrt{d})$ ,  $p_2 = 0.67$ , and the shell permittivities are matched to the transparency condition in Eqs. (7) and (14). Figure. (5), illustrates the RSL of the composite cloak, for

cylindrical dielectric and metal particles serving as an object. As expected, for systems with small overall sizes (see Fig 5(a) and 5(c)) a drastic reduction in scattering over the entire optical spectrum is achieved for  $\varepsilon_2 = (1 + p_2)/(1 - p_2)$ , thus reproducing the quasi-static result. Compared to a dielectric particle, a RSL across a broader frequency range is observed in the case of a metallic object. This is due to the dramatic enhancement of the metal particle scattering at the surface plasmon frequency  $\hbar\omega_{sp} = \hbar\omega_p/\sqrt{\varepsilon_b + \varepsilon_e} = 3.71\text{eV}$ . However, as the system size increases (see Fig 5(b) and 5(d)) the transparency condition in Eq. (7) is no longer sufficient to arrest the scattering process. This is an expected behavior since the contribution of the higher order multipoles in the scattering cross-length for  $k_e r_2 \ll 1$  increases with the physical size as (see Appendix)

$$S_n = \frac{i\pi}{\Gamma(n)\Gamma(n+1)} \left(\frac{k_e r_2}{2}\right)^{2n} \frac{\varepsilon_2(1 - p_2^n) - \varepsilon_e(1 + p_2^n)}{\varepsilon_2(1 - p_2^n) + \varepsilon_e(1 + p_2^n)} \quad (18)$$

It is straightforward to show that the quadruple scattering term of the cloak will overcome the dipolar term of the object for  $k_e r_2 > \sqrt{8p_1(1 + p_2 + p_2^2)}$  (assuming  $\varepsilon_0 \gg 1$ ). Overall, for particle diameters larger than 400 nm a substantial reduction in scattering/extinction cannot be expected in the optical spectral range.

Finally, we would like to address generic property of our cloak design, namely its object independence. The condition  $\varepsilon_{l-1} = 0$ , leads to  $\varepsilon_{eff}^{l-1} = 0$  (see Eq. (4)) regardless of the effective permittivity  $\varepsilon_{eff}^{l-2}$  of the underlying shell/object substructure. This allows the design to cloak virtually arbitrary in shape and composition objects provided the objects are encapsulated by  $l \geq 2$  shells.

To verify the generic properties of the cloak, full wave simulations using a finite-difference frequency domain (FDFD) software package (COMSOL Multiphysics) are performed.

A metallic rounded star shaped object is placed inside the cloak. The permittivities of the shells are set at  $\epsilon_2 = 5$  and  $\epsilon_1 = 0$  with radii ratio  $p_1 = 0.67$  ( $r_2 = 106$  nm and  $r_1 = 87$  nm). The system is illuminated by a TM polarized from a point source positioned 130 nm from the center of the object.

The magnetic field distribution is shown in Fig.6. The cylindrical wave generated by the source smoothly bends around the cloaked region indicating reduced scattering (see Fig. 6(a)). The phase fronts remain undisturbed as they exit the cloak and no shadow formation is noted. Figure 6(b) illustrates the magnetic field distribution when the cloak is removed. In this case the incident wave is strongly scattered and the phase fronts appear severely disturbed after traversing the object. The formation of shadows and presence of resonances within the object are clearly observed. The difference between the systems response shows that the cloak design based on the transparency condition Eq. (7) can considerably reduce scattering from objects with diverse optical and geometrical properties

## V. SUMMARY

In this work we propose a *generic cloaking system* based on zero-permittivity composite materials. The proposed analytical model and full wave calculations show that a dramatic suppression of dipolar scattering can be achieved for an arbitrary object enclosed within a multi-shell cloaking system. A reduction of scattering across the entire optical spectrum for dielectric objects using realistic shell materials is demonstrated. This study provides a new direction for achieving optical invisibility without the use of metamaterials and also underlines the role of zero-index materials in the general phenomenon of optical transparency.

## VI. APPENDIX

To calculate the scattering coefficients of the cloaking system shown in Fig. 1(b), we solve the Maxwell's curl equations in cylindrical coordinates. For an incident plane TM wave the

286 components of the incident field ( $i$ ), the field inside the  $m$ -th shell and scattered magnetic fields  
 287 assume the following general form

$$\begin{aligned}
 H_z^i &= H_0 \sum_{n=-\infty}^{\infty} i^n J_n(k_e r) e^{in\phi} \\
 H_z^{(m)} &= H_0 \sum_{n=-\infty}^{\infty} i^n [A_n^{(m)} J_n(k_m r) + B_n^{(m)} H_n^1(k_m r)] e^{in\phi}, \quad (A1) \\
 H_z^s &= H_0 \sum_{n=-\infty}^{\infty} i^n S_n H_n^1(k_e r) e^{in\phi}
 \end{aligned}$$

288 where  $J_n, H_n^1$  are the Bessel and Henkel functions of the first kind, respectively,  $k_e$  and  $k_m$   
 289 ( $m = 0, 1, 2, \dots, l$ ) are the wave numbers inside the cloak.  $A_n^{(m)}, B_n^{(m)}, S_n$  are the expansion  
 290 coefficients with  $B_n^{(0)} = 0$  at the origin. For an  $l$ -shell system, and applying boundary conditions,  
 291 the scattering coefficients (for  $\varepsilon_{l-1} = 0$ ) are given as

$$S_n^{cloak} = \frac{\alpha_n^l J_n(k_l r_{l-1}) + \beta_n^l H_n^1(k_l r_{l-1})}{\gamma_n^l J_n(k_l r_{l-1}) + \delta_n^l H_n^1(k_l r_{l-1})}, \quad (A2)$$

292 where  $k_l = (\omega/c)\sqrt{\varepsilon_l}$  and coefficients

$$\begin{aligned}
 \alpha_n^l &= \varepsilon_l J'_n(k_e r_l) H_n^1(k_l r_l) - \varepsilon_e J'_n(k_l r_l) J_n(k_e r_l) \\
 \beta_n^l &= \varepsilon_e J'_n(k_l r_l) J_n(k_e r_l) - \varepsilon_l J'_n(k_e r_l) J_n(k_l r_l) \\
 \gamma_n^l &= \varepsilon_e H_n^1(k_l r_l) H_n^1(k_e r_l) - \varepsilon_l H_n^1(k_e r_l) H_n^1(k_l r_l) \\
 \delta_n^l &= \varepsilon_l H_n^1(k_e r_l) J_n(k_l r_l) - \varepsilon_e J'_n(k_l r_l) H_n^1(k_e r_l).
 \end{aligned} \quad (A3)$$

293 Here the prime correspond to differentiation with respect to the radial coordinate and special care  
 294 must be taken when considering the  $n = 0$  term. Similarly, the scattering coefficients for the  
 295 object are

$$S_n^{obj} = \frac{\varepsilon_e J'_n(k_0 r_0) J_n(k_e r_0) - \varepsilon_0 J'_n(k_e r_0) J_n(k_0 r_0)}{\varepsilon_0 H_n^1(k_e r_0) J_n(k_0 r_0) - \varepsilon_e J'_n(k_0 r_0) H_n^1(k_e r_0)}. \quad (A4)$$

296 In the quasistatic limit  $k_l r_l \ll 1$ , Eqs. (A2) and (A4) are reduced to



$$\begin{aligned}
S_n^{cloak} &= \frac{i\pi}{\Gamma(n)\Gamma(n+1)} \left( \frac{k_e r_l}{2} \right)^{2n} \left( \frac{\varepsilon_l(1 - p_l^n) - \varepsilon_e(1 + p_l^n)}{\varepsilon_l(1 - p_l^n) + \varepsilon_e(1 + p_l^n)} + O[(k_e r_l)^2] \right) \\
S_n^{obj} &= \frac{i\pi}{\Gamma(n)\Gamma(n+1)} \left( \frac{k_e r_0}{2} \right)^{2n} \left( \frac{\varepsilon_0 - \varepsilon_e}{\varepsilon_0 + \varepsilon_e} + O[(k_e r_0)^2] \right).
\end{aligned} \tag{A5}$$

297 Considering the dipolar term ( $n = 1$ ) we derive the second transparency condition for the cloak

$$\varepsilon_l = \varepsilon_e \frac{1 + p_l}{1 - p_l}, \tag{A6}$$

298 which coincides with Eq. (7b) for  $d = 2$ . We must note that elimination of an arbitrary multipole

299 ( $n$ ) can also be eliminated from the far field provided

$$\varepsilon_l = \varepsilon_e \frac{1 + p_l^n}{1 - p_l^n}. \tag{A7}$$

300

301

### Acknowledgements

302 We would like to thank Dr. S.G Moiseev, K. Inturi, S. Animilli, Dr. N. Simicevic, Dr. A.

303 Sihvola and Dr. D. Robbins for useful discussions. This work has been supported by

304 the Louisiana Board of Regents and NSF under contract numbers LEQSF (2007-12)-ENH-

305 PKSFI-PRS-01, LEQSF(2011-14)-RD-A-18 and NSF(2010)-PFUND-202.

306

307

308

309

310

311

### REFERENCES

312 <sup>1</sup>W. Cai, U. K. Chettiar, A. V. Kildishev, and V. M. Shalaev, Nature Photonics **1**, 224 (2007).

313 <sup>2</sup>S. A. Cummer, B. I. Popa, D. Schurig, D. R. Smith, and J. Pendry, Phys. Rev. E **74**, 036621  
314 (2006)

- 315 <sup>3</sup>U. Leonhardt, Science **312**, 1777 (2006).
- 316 <sup>4</sup>J. B. Pendry, D. Schurig, and D. R. Smith, Science **312**, 1780 (2006).
- 317 <sup>5</sup>U. Leonhardt and T. Philbin, Geometry and Light: The Science of Invisibility, (Dover, Newyork
- 318 2010).
- 319 <sup>6</sup>U. Leonhardt and T. Philbin, New J. Phys. **8**, 247 (2006).
- 320 <sup>7</sup>Y. Lai, H. Chen, Z-Q. Zhang, and C. T. Chan, Phys. Rev. Lett. **102**, 093901 (2009)
- 321 <sup>8</sup>J. B. Pendry and S. A. Ramakrishna, J. Phys. Condens. Matter **14**, 8463 (2002)
- 322 <sup>9</sup>H. Chen<sup>1</sup>, C. T. Chan and P. Sheng, Nature Materials **9**, 387 (2010)
- 323 <sup>10</sup>M. W. McCall, A. Favaro, P. Kinsler, A. Boardman, J. Opt. **13**, 024003 (2011)
- 324 <sup>11</sup>D. Schurig, J. Mock, B. Justice, S. Cummer, J. Pendry, A. Starr, and D. Smith, Science **314**,
- 325 977 (2006)
- 326 <sup>12</sup>Y. Huang, Y. Feng, and T. Jiang, Opt. Express **15**, 11133 (2007).
- 327 <sup>13</sup>J. Valentine, S. Zhang, T. Zentgraf, E. Ulin-Avila, D. Genov, G. Bartal, and X. Zhang, Nature
- 328 **455**, 376 (2008).
- 329 <sup>14</sup>N. Fang, H. Lee, C. Sun, and X. Zhang, Science **308**, 534 (2005).
- 330 <sup>15</sup>Y. Lai, J. Ng, HY Chen, D Han, J. Xiao, Z-Q Zhang, and C. T. Chan, Phys. Rev. Lett. **102**,
- 331 253902 (2009)
- 332 <sup>16</sup>D. A. Genov, S. Zhang, and X. Zhang, Nature Phys. **5**, 687 (2009).
- 333 <sup>17</sup>A. Alù and N. Engheta, Phys. Rev. E **72**, 016623 (2005).
- 334 <sup>18</sup>M. Kerker, J. Opt. Soc. Am. **65**, 376 (1975).
- 335 <sup>19</sup>X. Zhou and G. Hu, Phys. Rev. E **74**, 026607 (2006)
- 336 <sup>20</sup>P. Alitalo, O. Luukkonen, L. Jylha, J. Venermo, and S. A. Tretyakov, IEEE. Trans. Antennas
- 337 and Propag. **56**, 416 (2008).
- 338 <sup>21</sup>G. W. Milton and N.-A. P. Nicorovici, Proc. R. Soc. A **462**, 3027 (2006).
- 339 <sup>22</sup>E. Palik, Handbook of Optical Constants of Solids, (Academic Press, London,1997).
- 340 <sup>23</sup>N. Garcia, E. V. Ponizovskaya, and J. Q. Xiao, Appl. Phys. Lett. **80**, 1120 (2002).
- 341 <sup>24</sup>D. J. Bergman and D. Stroud, Physical Properties of Macroscopically Inhomogenous Media, in
- 342 Solid State Physics, Vol. 46 (Academic Press, Inc., 1992).
- 343 <sup>25</sup>D. A. Genov, A. K. Sarychev, and V. M. Shalaev, J. Nonlinear Opt. Phys. Mater **12**, 419
- 344 (2003).
- 345 <sup>26</sup>J. C. Maxwell-Garnett, Philos. Trans. R. Soc. London **203**, 385 (1904).
- 346 <sup>27</sup>D. Polder and J. Vansantenn, Physica **12**, 257 (1946).
- 347 <sup>28</sup>C. Bohren and D. Huffman, Absorption and Scattering of Light by Small Particles, (Wiley,
- 348 New York, 1998).
- 349 <sup>29</sup>M. Kerker and E. Matijevi, J. Opt. Soc. Am. **51**, 506 (1961).
- 350 <sup>30</sup>G. Mie, Ann. Physik **330**, 377 (1908).

351

352

353

## Figures

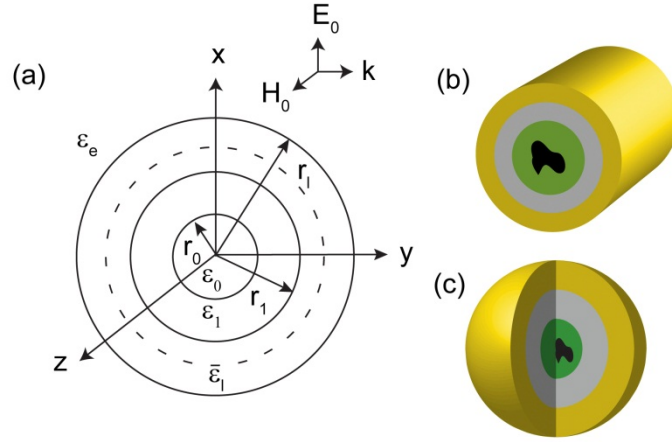


FIG. 1. (a) Generic multi-shell cloaking system with shell radii  $r_i$  and permittivity  $\epsilon_i$ , a two shell  
 (b) cylindrically symmetric cloaking system and (c) spherically symmetric cloaking system.

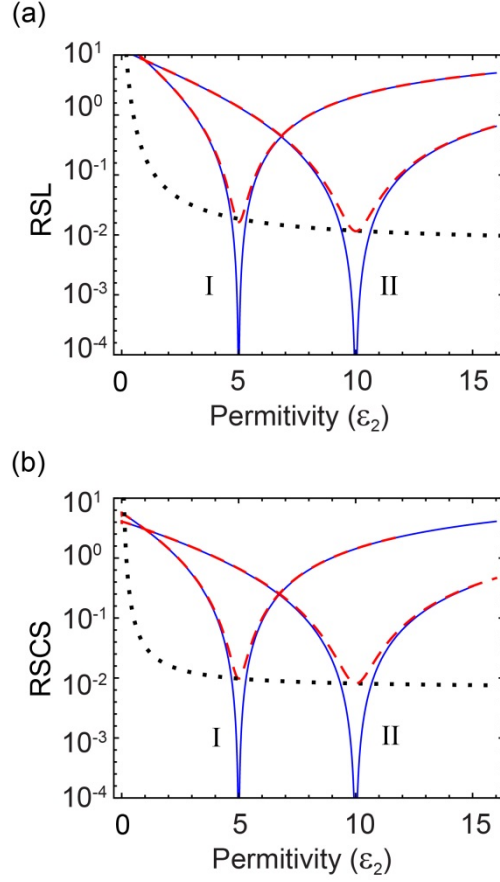


FIG. 2. Relative scattering length (RSL) and cross-section (RSCS) versus outer shell permittivity for two-shell (a) cylindrically symmetric cloak and (b) spherically symmetric cloak with inner shell made of bulk silver. Two separate designs are being investigated in case of cylindrical system: (I)  $p_2 = 0.67$  and (II)  $p_2 = 0.82$ , and spherical system (I)  $p_2 = 0.73$  and (II)  $p_2 = 0.86$ . The object permittivity is  $\epsilon_0 = 12$  and for all cases we use the optimal radii ratio  $p_1 = 1/(1 + \sqrt{d})$ . The limiting case as per Eq. (10) is presented with dotted (black) lines.

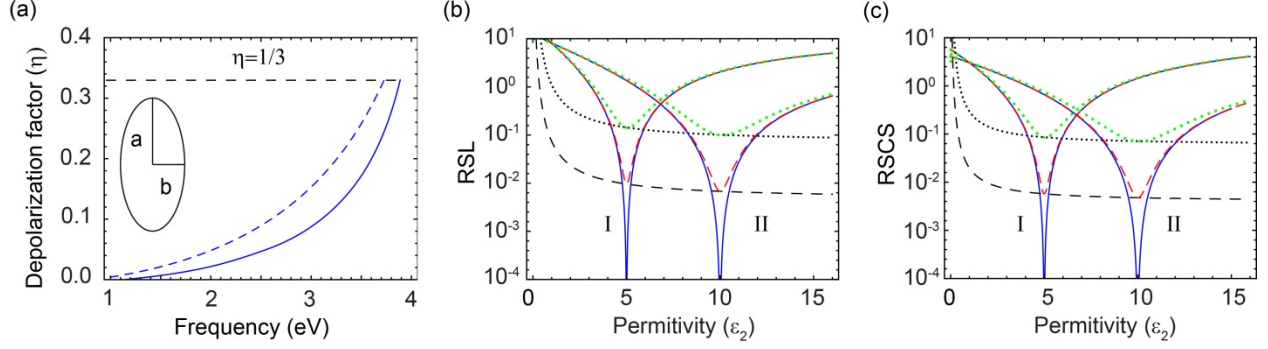


FIG. 3. (a) Depolarization factor for composite host materials  $\epsilon_h = 1$  (solid line) and  $\epsilon_h = 2.0$  (dashed line) at different frequencies and  $f = 0.05$ . Relative scattering length (RSL) and cross-section (RSCS) versus outer shell permittivity of two-shell (b) cylindrically symmetric cloaking system and (c) spherically symmetric cloaking system, respectively. The composite inner shell is designed with two different hosts  $\epsilon_h = 1$  (dashed red line) and  $\epsilon_h = 2.0$  (dotted green line) at  $\hbar\omega = 1.14$  eV. In the plots we also consider two separate shell designs; cylindrical system (I)  $p_2 = 0.67$  and (II)  $p_2 = 0.82$ , and spherical system (I)  $p_2 = 0.73$  and (II)  $p_2 = 0.86$ . The embedded object has permittivity  $\epsilon_0 = 12$  and for all cases we use the optimal shell radii ratio  $p_1 = 1/(1 + \sqrt{d})$ . The ideal lossless cases are represented with solid (blue) lines. The limiting case (as per Eqs. (9) and (14)) is presented with horizontal (dotted and dashed) black lines for both the host media.

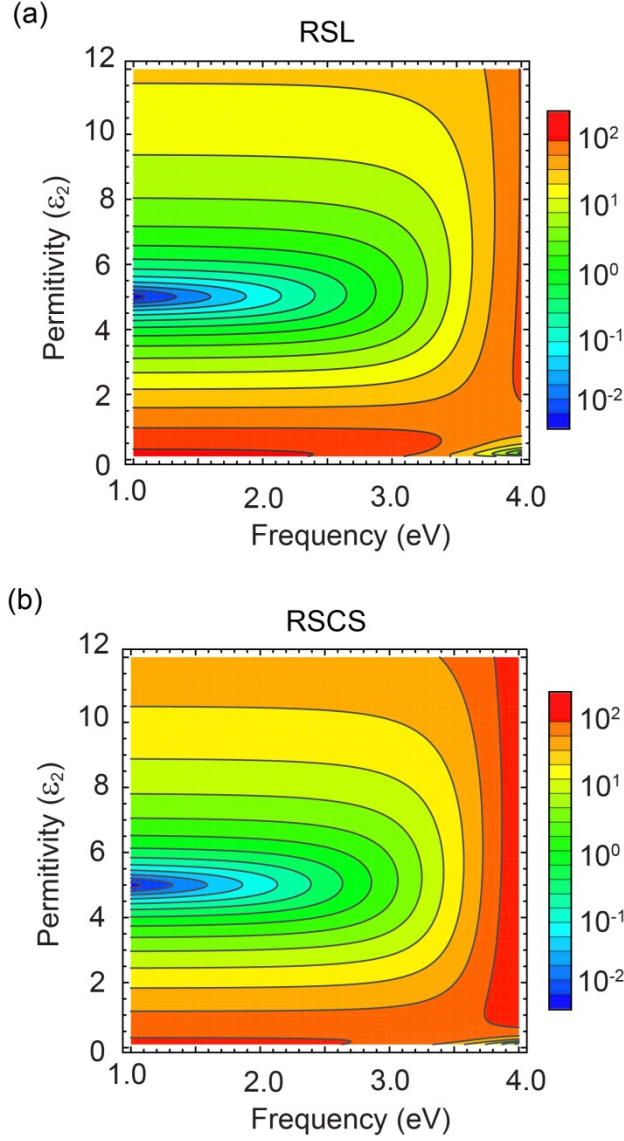


FIG. 4. (a) Relative scattering length (RSL) and (b) relative scattering cross-section (RSCS) calculated as function of outer-shell permittivity ( $\epsilon_2$ ) and incident light frequency for a dielectric particle ( $\epsilon_0 = 12$ ) with  $\epsilon_h = 1$  and spheroids volume/surface fraction  $f = 0.05$ . The shells radii ratios are (a) cylindrical system  $(p_1, p_2) = (0.41, 0.67)$ , and (b) spherical system  $(p_1, p_2) = (0.37, 0.73)$ .

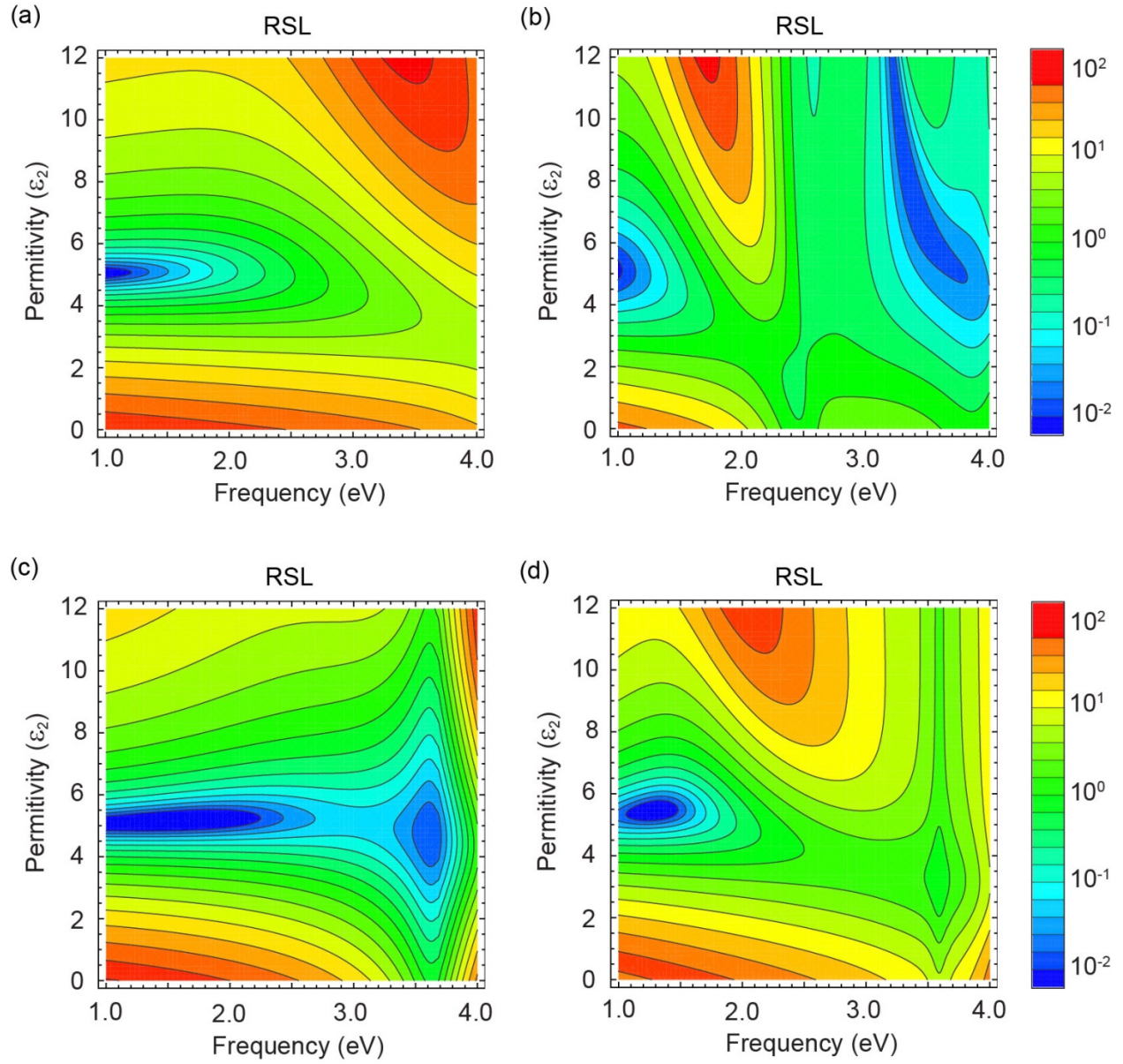


FIG. 5. Full wave calculations of the relative scattering length (RSL) as function of outer shell permittivity ( $\epsilon_2$ ) and incident light frequency for dielectric particle  $\epsilon_0 = 12$  (a, b) and metal particle (c, d) enclosed in a cloaking system with radii  $r_2 = 50$  nm (a, c) and  $r_2 = 100$  nm (b, d).



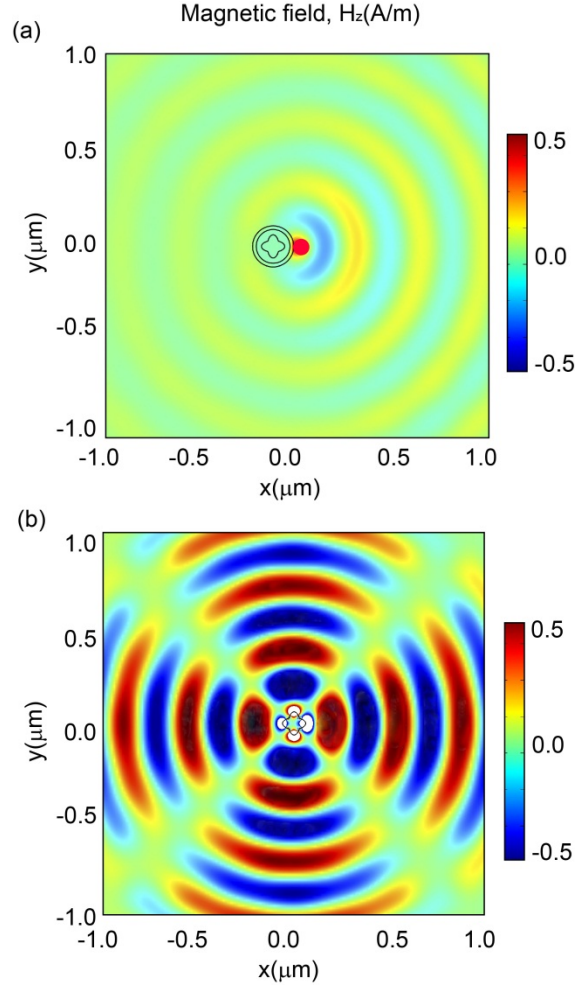


FIG. 6. Full wave calculations of light scattering due to a point source in close proximity to a star shaped metal object with (a), and without (b) the cloak. The incident TM wave has frequency  $\hbar\omega = 3.8$  eV.